Featured Article

Persistent Activation of the Akt Pathway in Head and Neck Squamous Cell Carcinoma: A Potential Target for UCN-01

Panomwat Amornphimoltham,[1] Virote Sriuranpong,[1] Vyomesh Patel,[1] Fernando Benavides,[2] Claudio J. Conti,[2] John Sauk,[3] Edward A. Sausville,[4] Alfredo A. Molinolo,[1] and J. Silvio Gutkind[1]

[1]Oral and Pharyngeal Cancer Branch, National Institute of Dental and Craniofacial Research, NIH, Bethesda, Maryland; [2]Department of Carcinogenesis, The University of Texas M. D. Anderson Cancer Center, Smithville, Texas; [3]Department of Diagnostic Science and Pathology, Dental School, University of Maryland, Baltimore, Maryland; and [4]Developmental Therapeutics Program, National Cancer Institute, NIH, Rockville, Maryland

ABSTRACT

Squamous carcinomas of the head and neck (HNSCC) represent the sixth most common cancer among men worldwide and a major cause of morbidity and mortality due to its relatively poor prognosis. As part of ongoing studies addressing the molecular events underlying tumor progression in HNSCC, we have explored the nature of the proliferative pathways in which dysregulation may promote aberrant cell growth in this tumor type. The serine/threonine protein kinase Akt is a downstream target of phosphatidylinositol 3-kinase and a key regulator of normal and cancerous growth and cell fate decisions. Therefore, in this study, we have examined the status of activation of Akt in different stages of squamous cell carcinoma development in mice and in clinical samples from HNSCC patients. By immunohistochemical analysis, using a recently developed phosphorylation state-specific antibody, we demonstrated that Akt activation correlates closely with the progression of mouse skin squamous cell carcinoma. We also observed that activation of Akt is a frequent event in human HNSCC because active Akt can be detected in these tumors with a pattern of expression and localization correlating with the progression of the lesions. In line with these observations, Akt was constitutively activated in a large fraction of HNSCC-derived cell lines. We also provide evidence that the Akt signaling pathway may represent a biologically relevant target for a novel antineoplastic agent, UCN-01, which recently has been shown to be active in cellular and xenograft models for HNSCC at concentrations safely achievable in clinically relevant situations.

INTRODUCTION

With >500,000 cases diagnosed each year, squamous carcinomas of the head and neck (HNSCC) represent the sixth most common cancer among men and a major cause of morbidity and mortality worldwide (1, 2). Indeed, the prognosis of advanced HNSCC patients is relatively poor, and its overall 5-year survival, ~50%, has not improved over the past three decades. However, current efforts exploring the molecular events underlying HNSCC tumor progression may soon afford the opportunity to identify molecular markers of diagnostic and prognostic value, as well as novel therapeutic targets in this particular cancer type. In general, the transformation of normal epithelium to squamous cell carcinoma (SCC) occurs in multiple steps, involving the sequential activation of oncogenes and inactivation of tumor suppressor genes (3). Although remarkable progress has been made recently in the identification of the alteration of tumor suppressor genes and their related protein products in HNSCC (3), the nature of the proliferative pathways driving uncontrolled cell growth in this tumor type are still poorly defined, thus limiting our ability to identify mechanism-based therapeutic approaches for this disease.

The serine/threonine protein kinase Akt, also known as PKB, is a downstream target of phosphatidylinositol 3′-kinase (PI3K) and has been shown to be a key regulator of various cellular processes, including normal and aberrant cell growth and cell fate decisions such as differentiation and cell survival or death by apoptosis (4, 5). Activated Akt has been shown to be a frequent event in several cancer types such as breast (6), colorectal (7), and ovarian (8) cancer. Of interest, using a mouse model for chemically induced squamous carcinoma, we have recently observed that elevation in the kinase activity of Akt represents an early event during the papilloma formation that precedes squamous carcinogenesis (9). Furthermore, using cell grafting analysis, we provided evidence that activated Akt accelerates tumor progression and promotes the malignant conversion of immortalized murine keratinocyte cell lines (9).

These observations prompted us to examine the status of activation of Akt in clinical samples from HNSCC patients. Initially, we confirmed that Akt is activated in mouse skin SCC by a recently developed immunohistochemical analysis using phosphorylation state-specific antibodies that recognized Akt when phosphorylated in position Ser^{473}, which represents the active form of this kinase. Furthermore, we observed that activation of Akt is a frequent event in human HNSCC because active Akt can be detected in these tumors with a pattern of expression and localization correlating well with the progression of the lesions. In line with these observations, Akt was constitutively phosphorylated and its kinase activity elevated in a large fraction of HNSCC-derived cell lines. We also provide evidence that the Akt signaling pathway may represent a bio-

Received 9/17/03; revised 3/17/04; accepted 3/18/04.
The costs of publication of this article were defrayed in part by the payment of page charges. This article must therefore be hereby marked *advertisement* in accordance with 18 U.S.C. Section 1734 solely to indicate this fact.
Requests for reprints: J. Silvio Gutkind, Oral and Pharyngeal Cancer Branch, National Institute of Dental and Craniofacial Research, NIH, 30 Convent Drive, Building 30, Room 212, Bethesda, MD 20892-4330. Phone: (301) 496-6259; Fax: (301) 402-0823; E-mail: sg39v@nih.gov.

logically relevant target for a novel antineoplastic agent, UCN-01, which has been recently shown to be active in cellular and xenograft models for HNSCC at concentrations safely achievable in clinically relevant situations.

MATERIALS AND METHODS

Human Tissues. Formalin-fixed, paraffin-embedded tissue specimens from head and neck cancer patients were retrieved from the archives of Department of Diagnostic Science and Pathology, Dental School, University of Maryland, with the approval of the Institutional Review Board. All tissues were stained H&E for pathological diagnosis. The tissues were divided, according to their histology, into four distinct groups: normal/metaplastic epithelium, which included normal epithelium adjacent to more advanced lesions; dysplasias; carcinomas *in situ*; and invasive SCCs.

Mouse Tissues. Samples of normal mouse skin, hyperplasia, papilloma and SCC were obtained from SENCARB mice using the two-stage skin carcinogenesis model by treated with 7,12-dimethylbenz(*a*)anthracene and 12-*O*-tetradecanoylphorbol-13-acetate as previously described (10) in accordance with approved animal protocols. Tissues were snap-frozen or fixed in buffered formalin and embedded in paraffin. Five-μm sections were obtained and stained with H&E for diagnostic purposes or left unstained for immunocytochemistry.

Antibodies. Rabbit polyclonal phospho-Akt (Ser^{473}) immunohistochemistry (IHC)-specific antibody (Cell Signaling Technology, Beverly, MA; dilution 1:50) was used for IHC; rabbit polyclonal phospho-Akt ($Ser^{472/473/474}$; BD PharMingen), rabbit polyclonal Akt antibody (BD PharMingen), mouse monoclonal glycogen synthase kinase-3β (GSK-3β; BD PharMingen), rabbit polyclonal phospho-mTOR (Ser^{2448}; Cell Signaling Technology), rabbit polyclonal mTOR antibody (Cell Signaling Technology), and rabbit polyclonal phospho-GSK-3 α/β ($Ser^{21/9}$; Cell Signaling Technology) were used for Western blotting at a dilution 1:1000.

IHC. The tissues slides were dewaxed in xylene, hydrated through graded alcohols and distilled water, and washed with PBS. Antigen retrieval was performed using a commercial unmasking solution (Vector Laboratories, Burlingame, CA) in a microwave for 20 min (2 min at 100% power and 18 min at 10% power). Slides were allowed to cool down for 30 min at room temperature, rinsed twice with PBS, and incubated in 3% hydrogen peroxide in PBS for 30 min to quench the endogenous peroxidase. The sections were then washed in distilled water and PBS and incubated in blocking solution (5% horse serum) for 1 h at room temperature. Excess solution was discarded, and the sections incubated with the primary antibody diluted in blocking solution at 4°C overnight. After washing with PBS, the slides were sequentially incubated with the biotinylated secondary antibody (1:300; Vector Laboratories) for 1 h, followed by the avidin-biotin complex method (Vector Stain Elite, ABC kit; Vector Laboratories) for 30 min at room temperature. The slides were washed and developed in 3,3′-diaminobenzidine (Sigma FASTDAB tablet; Sigma Chemical, St. Louis, MO) under microscopic control. The reaction was stopped in tap water, and the tissues were counterstained with Mayer's hematoxylin, dehydrated, and mounted. To capture the entire areas of interest, several partially overlapping high-definition images were taken from each case with a total magnification of ×160, using a real-time Retiga 1300 digital camera with the QImaging Pro software (MVIA, Inc., Monaca, PA). The images were then stitched together using the PanaVue Image Assembler Software (PanaVue Co., Quebec City, Quebec, Canada). The resulting image was a high-quality panoramic picture of the lesion that allowed us to analyze simultaneously a high number of positively and negatively stained cells, frequently including within the same section, nonneoplastic reactive epithelium, as well as different degrees of tumor progression, which were analyzed under the same software parameters. Images were quantified using the Northern Eclipse Image Analysis Software (Empix Imaging, North Tonawanda, NY) and expressed as the percentage of phospho-Akt (*p*-Akt)-positive cells with respect to the total number of cells in each histologically defined area.

Immunocytochemistry. Cells were grown on the coverslips until 50% confluent, serum-starved, subjected to different experimental conditions, and washed twice in cold PBS. Coverslips were immersed in 100% methanol at −20°C for 10 min and washed twice in cold PBS.

Blocking step, antibody incubation, and staining conditions were all performed as described in IHC.

Cells Cultures. HNSCC cell lines HN4, HN6, HN8, HN12, HN13, HN17, HN19, HN22, HN26, HN30, and HN31 and HaCaT cells were maintained in DMEM with 10% FCS, penicillin, and streptomycin in 5% CO_2 at 37°C as described previously (11).

Pharmacological Treatment. UCN-01 was provided by Kyowa Hakko Kogyo Co. Ltd., Japan, to the Development Therapeutics Program, National Cancer Institute. The compound was reconstituted in DMSO as a 10 mM stock solution, which was additionally diluted to the working concentration in culture medium (1–1000 nM), at a final concentration of ≤0.1%. Epidermal growth factor (EGF) was purchased from Sigma Chemical and used as indicated (100 ng/ml for 10 min). Wortmannin was purchased from Calbiochem (San Diego, CA) and used at a concentration of 50 nM.

Western Blotting. Cells were rinsed twice in PBS, lysed with protein lysis buffer [62.5 mM Tris-HCl (pH 6.8), 2% v/v SDS, and 50 mM DTT], scraped immediately, and transferred to microcentrifuge tubes. Lysate was sonicated for 20 s. The protein yield was quantified using the DC protein assay kit (Bio-Rad, Hercules, CA). Equivalent amounts of protein (50 μg) were separated by SDS-PAGE and then transferred to polyvinylidene difluoride membranes. Equivalent loading was confirmed by staining membranes with Ponceau-S. The membranes were blocked for 1 h in blocking buffer (1× Tris-buffered saline, 5% nonfat dry milk, and 0.1% Tween 20), which was then replaced by the primary antibody at the concentration described above, in blocking buffer, overnight at 4°C. After incubation, the membranes were washed three times in washing buffer (1× Tris-buffered saline and 0.1% Tween 20). Primary antibody was detected using horseradish peroxidase-linked goat antimouse (Santa Cruz Biotechnology, Santa Cruz, CA) or goat antirabbit IgG antibody (Santa Cruz Biotechnology) and visualized with SuperSignal West Pico chemiluminescent substrate (Pierce, Rockford, IL). The bands were scanned and quantified using NIH image software.

Akt Kinase Assay. To assay for Akt kinase activity, cells were serum-starved, subjected to the different experimental conditions, washed twice in cold PBS, and lysed on ice with 500 μl of lysis buffer containing 20 mM Tris (pH 7.5), 150 mM NaCl, 1 mM EDTA, 1 mM EGTA, 1% Triton X-100, 2.5 mM Na PP_I, 1 mM β-glycerophosphate, 1 mM Na_3VO_4, 1 μg/ml leupeptin, and 1 mM phenylmethylsulfonyl fluoride. Equal amounts of lysates (300 μg of protein) were precleared by centrifugation and preabsorbed with protein A-protein G (1:1) agarose slurry. Immunoprecipitation was carried out for 18 h using an immobilized anti-Akt1G1 monoclonal antibody cross-linked to agarose. Immunoprecipitates were washed three times with lysis buffer and twice with Akt kinase buffer (25 mM Tris (pH 7.5), 5 mM β-glycerophosphate, 2 mM DTT, 0.1 mM Na_3VO_4, and 10 mM $MgCl_2$). Kinase assays were performed for 30 min at 30°C under continuous agitation in kinase buffer containing 200 μM ATP and 1 μg of GSK-3 fusion protein as a substrate, according to the manufacturer's instructions (Cell Signaling Technology). The incorporation of phosphate into GSK-3 was assessed by Western blot using an antiphospho-specific GSK-3 α/β ($Ser^{21/9}$) antibody and horseradish peroxidase-conjugated antirabbit antibody. To assess the level of expression of Akt, parallel total cell lysates were analyzed by Western blot, using a polyclonal goat antibody against human Akt.

Cell Proliferation. [^{3}H]Thymidine (ICN Pharmaceuticals, Inc., Costa Mesa, CA) uptake was performed as described previously (12). Briefly, HNSCC and HaCaT cells (1–2 × 10^4/well) were allowed to attach overnight in 24-well plates, and the medium was replaced with serum-free medium 24 h for the vehicle control wells. After treatment (20 h), the cells were pulsed with [^{3}H]thymidine (1 μCi/well) for 4 h, precipitated DNA (5% trichloroacetic acid), and solubilized (0.5 M NaOH) before scintillation counting. Experiments were performed in triplicate.

Statistical Analysis. ANOVA followed by the Turkey *t* test was used to analyze the differences between groups after immunohistochemical staining of human HNSCC for *p*-Akt protein. Data analysis was performed with using GraphPad Prism version 4.00 for Windows, GraphPad Software, San Diego, CA;[5] P values < 0.05 were considered statistically significant.

RESULTS

Detection of Activated Akt in Mouse Tissues. The recent development of new immunological tools detecting the phosphorylated form of Akt, which represents its activated state (13), provides a unique opportunity to monitor the activation of Akt in tissue sections, thereby facilitating the analysis of its status in defined cell populations and even subcellular locations within a tumor. Fig. 1 shows the expression of *p*-Akt detected by IHC in normal or pathological tissue from SENCARB mice under the two-step chemically induced carcinogenesis treatment (10). Expression of the activated form of Akt correlated with SCC progression, paralleling our prior enzymatic analysis of

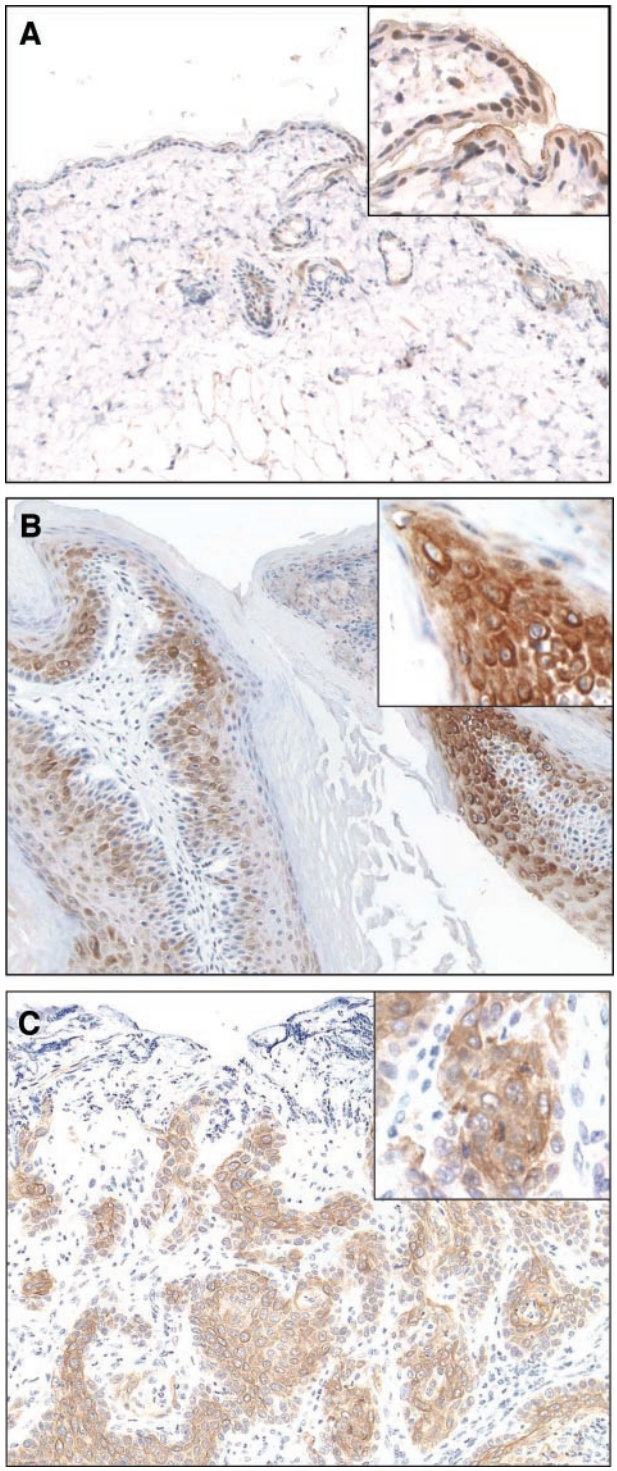

Fig. 1 *A*, phospho-Akt (*p*-Akt) staining in normal mouse skin. Isolated positive cells can be seen scattered in the epidermis (×200). *Inset:* moderate cytoplasmic or nuclear staining in normal epithelial cells (×400). *B*, papilloma; *p*-Akt-positive staining is evident in the lower third of the hyperplastic squamous epithelium (×200). *Inset:* strong cytoplasmic staining of ~100% of the cells in this area (×400). *C*, infiltrating SCC; most neoplastic malignant keratinocytes are positive for *p*-Akt (×200). *Inset:* staining distribution is cytoplasmic in all malignant cells (×400).

[5] Internet address: http://www.graphpad.com.

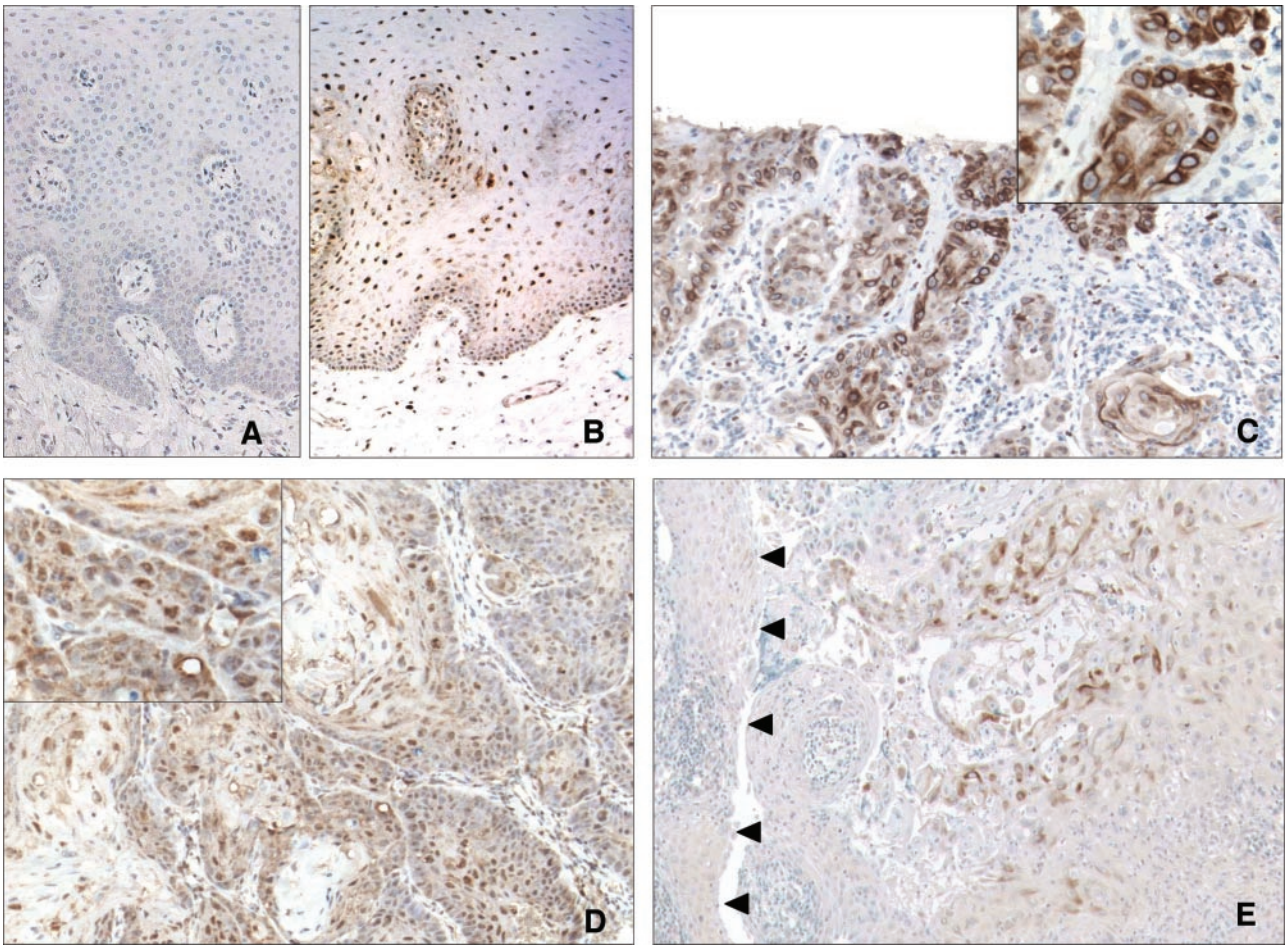

Fig. 2 *A*, normal oral mucosa exhibits only mild phospho-Akt (*p*-Akt) staining in isolated cells in the basal epithelial layer. *B*, predominant nuclear staining for *p*-Akt in the lower half of the squamous epithelium in a mild dysplasia of the oral mucosa. Note positive immunoreactivity in isolated fibroblastic-like stromal cells and endothelial cells. *C* and *D*, two squamous carcinomas of the head and neck showing different *p*-Akt immunoreactivity distribution patterns; staining in *C* is almost exclusively cytoplasmic, whereas *D* presents extensive cytoplasmic as well as nuclear positive staining. *E*, *p*-Akt staining in squamous carcinoma of the head and neck, showing positive staining in the cytoplasm of the invasive front of squamous cell carcinoma, whereas only very mild staining for *p*-Akt can be observed in the normal adjacent cells (*arrowheads*).

Akt activity (9). Normal skin exhibited only isolated nuclear staining in basal cells of skin and hair follicles (Fig. 1*A*). The intensity and number of positive cells for *p*-Akt increased dramatically in skin papillomas, where cytoplasmic staining was observed in every sample (Fig. 1*B*). At the carcinoma stage, almost all cells showed cytoplasmic immunoreactivity for *p*-Akt, which was even stronger in invasive areas (Fig. 1*C*).

Accumulation of Phospho-Akt in Human HNSCC. Because the immunodetection of *p*-Akt in mouse SCC correlated well with the enhanced Akt activity in these tissues (9), these findings prompted us to evaluate the status of Akt activation in human HNSCC using the IHC approach. Indeed, we found that human HNSCC exhibited a similar pattern of expression of *p*-Akt, which correlated with disease progression (Figs. 2 and 3). In normal tissues, the staining was limited to few cells (Figs. 2 and 3) within the basal or parabasal layers and almost always confined to the cell nucleus. The image was similar in metaplastic or inflammatory areas, although the percentage of stained cells was marginally higher. Focal cytoplasmic staining could be seen in normal squamous epithelium adjacent to dysplastic or malignant lesions. In dysplastic areas, a high fraction of the cells presented with strong nuclear staining (Figs. 2 and 3). Carcinoma *in situ* also presented with strong nuclear staining, as well as *p*-Akt staining in the cytoplasm. Only in a few cases was nuclear staining observed in invasive lesions; in most instances, *p*-Akt staining was predominantly cytoplasmic (Fig. 2, *C–E*), a staining pattern similar to that observed in mouse tissues. The percentage of positively stained cells among the different groups showed significant differences between normal/metaplasia to dysplasia ($P < 0.001$), carcinoma *in situ* ($P < 0.01$), or SCC ($P < 0.05$).

Constitutive Active Akt in HNSCC. To further control the experimental conditions used to examine active Akt in tissues, we used the same IHC conditions for the immunocytochemical analysis of *p*-Akt in a more defined cellular system *in vitro*. Indeed, using HaCaT cells, an immortalized human epidermal cell line, we observed that there was limited *p*-Akt staining under basal conditions but that treating with EGF (100

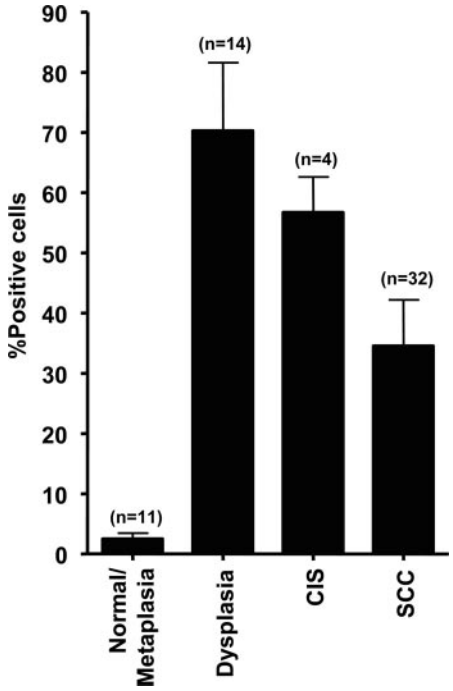

Fig. 3 Quantitative analysis of immunohistochemistry: data are representing the percentage of positively staining cells observed in normal and metaplasia, dysplasia, carcinoma *in situ* (CIS), and invasive squamous carcinoma (SCC), compared with total cells present in each histologically defined area. Number of cases analyzed is indicated in parenthesis.

ng/ml for 10 min) dramatically enhanced *p*-Akt immunoreactivity (Fig. 4*A*). On the contrary, treatment with wortmannin (50 nM 30 min), a potent PI3K inhibitor (14), can abolish basal *p*-Akt staining and diminished the *p*-Akt response to EGF (Fig. 4*A*). These observations were additionally confirmed by the parallel Western blot analysis of cell lysates using a distinct *p*-Akt antibody that recognizes the phosphorylation of $Ser^{472/473/474}$ of all Akt isoforms. As shown in Fig. 4*B*, there was a remarkably high level of *p*-Akt when cells were treated with EGF, which was inhibited by the treatment with wortmannin without affecting the total level of Akt protein. Enhanced *p*-Akt levels correlated with increased Akt kinase activity, as judged by immunocomplex Akt kinase reactions using GSK3α/β as a biologically relevant substrate *in vitro* (Fig. 4*B*).

We then investigated whether the increased Akt activity observed in human HNSCC was reflected in Akt activation in HNSCC-derived cells lines. For this analysis, we selected a panel of 11 HNSCC cell lines derived from primary and secondary cancer lesions of contrasting clinical staging (11). These cells have been comprehensively explored for alterations of major tumor suppressor genes (15, 16). For example, aberrant forms of *p53* and $p16^{INK4A}$ were presented in all of the cell lines tested with the exception of one, HN30, which was found to express wild-type *p53*, thus displaying normal p53 function (16). Accordingly, we performed Western blot analysis using a *p*-Akt antibody in lysates from this panel of HNSCC cell lines (Fig. 4*C*). The majority of the HNSCC cells exhibited increased levels of active Akt, albeit to different extents. HN6 cells demonstrated the highest levels of constitutively active Akt among all of the cells examined, followed by HN12, HN13, and HN26, whereas HN17, HN19, and HN 31 displayed a moderate level of activation. By comparison, HN4, HN8, HN22, and HN30 cells had low level of constitutively active Akt (Fig. 4*C*). Total Akt levels were similar in all cells. The status of phosphorylation of Akt in these cells correlated tightly with their *in vitro* Akt enzymatic activity (Fig. 4*D* and data not shown).

UCN-01 Inhibits the PI3K-Akt Signaling Pathway in HNSCC. UCN-01 (7-hydroxystaurosporine) is a derivative of staurosporine, which was originally developed as an inhibitor of the protein kinase C family of serine-threonine kinases (17). This compound exhibits potent antiproliferative effects on a variety of tumor cells such as those derived from breast, lung, and colon in both *in vitro*, as well as *in vivo* experimental models (18–21). Furthermore, in a recent study, we have shown that UCN-01 effectively inhibits the growth of HNSCC cells and HNSCC tumor xenografts (12). Indeed, when we extended these original observations to the full panel of HNSCC cells used in this study, we observed that UCN-01 inhibits the incorporation of [^{3}H]thymidine into DNA in all HNSCC cells, with an EC_{50} ranging from 6 to 30 nM (data not shown). However, recent studies have revealed that the antiproliferative and proapoptotic activities of UCN-01 do not correlate with the blockade of protein kinase C (22). Instead, UCN-01 has been shown to inhibit other kinases important in cell cycle regulation, including Chk1 (23) and, indirectly, the cyclin-dependent kinases, the latter occurring through increases in the level of expression of the endogenous cyclin-dependent kinase inhibitors $p21^{WAF1}$ and $p27^{KIP1}$ (12).

Of interest, in a very recent study it was shown that UCN-01 can also block PDK1, a kinase that acts directly upstream of Akt (24). On the basis of the antiproliferative effect of UCN-01 in HNSCC cells and the fact that these cells exhibit hyperactive Akt, we next examined whether UCN-01 could inhibit the activity of Akt in these cells at concentrations that are consistent with the growth inhibitory effect of this compound at concentrations compatible with those achieved in tissues during recent clinical trials (25). As shown in Fig. 5*A*, UCN-01 potently decreased the levels of active Akt in a dose-dependent manner in HNSCC cells. Using as an example HN6, the EC_{50} for Akt inhibition was ~19 nM (range, 8–45 nM; $n = 4$), which corresponded well with the antiproliferative property of UCN-01 in these cells when assessed by [^{3}H]thymidine incorporation (EC_{50} ~7 nM). Furthermore, using a concentration of UCN-01 of 100 nM (EC_{90}), we observed that the activity of Akt in cells exhibiting high levels of constitutively active Akt decreased rapidly in a time-dependent manner, in most cases at least by 50–90% in ~30 min (Fig. 5*B*). In contrast, UCN-01 did not decrease but instead increased the activity of a distinct signaling route that leads to activation of extracellular signal-regulated kinases, as previously reported (22, 26), thus supporting the specificity of this effect on the Akt pathway.

We next evaluated whether the inhibition of the Akt pathway by UCN-01 was reflected by the decreased phosphorylation of endogenous Akt substrates. We focused our attention on GSK-3, which was initially identified as an enzyme that regulates glycogen synthesis, and was recently shown to be a critical

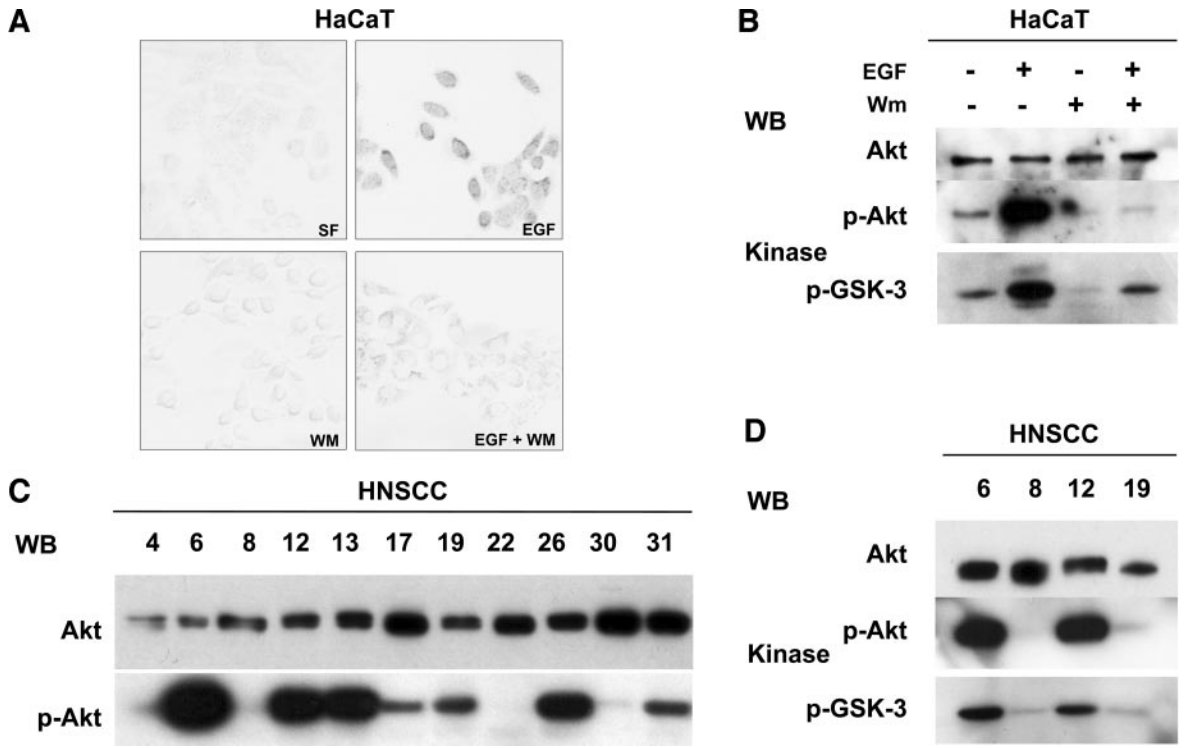

Fig. 4 Activated Akt is frequently found in squamous carcinoma of the head and neck (HNSCC) cell lines. *A* and *B*, immunostaining for phospho-Akt (*p*-Akt) correlates with the level of phosphorylated Akt and its *in vitro* kinase activity. *A*, serum-starved HaCaT cells were treated with epidermal growth factor (EGF; 100 ng/ml for 10 min) with or without pretreatment with wortmannin (WM; 50 nM, 30 min). Immunocytochemical analysis was performed as described in "Materials and Methods." *B*, cell lysates from cells treated as in *A* were processed for Western blotting (WB) with anti-Akt (Akt), or with phosphorylation-specific anti-Akt antibodies (*p*-Akt). *In vitro* immunocomplex Akt kinase reactions were performed and the phosphorylated product glycogen synthase kinase-3 (*p*-GSK-3) revealed with a phospho-specific GSK-3α/β antibody. *C*, expression pattern of *p*-Akt in HNSCC cells. Cell lysates were harvested from serum-deprived HNSCC cells. Immunoblotting for total Akt was performed in the same filter. *D*, immunocomplex Akt kinase assays were performed in HNSCC cell lines as described in *B*. A representative group is shown.

downstream element of PI3K/Akt cell survival pathway (27). Using HN6 as an example, we observed that UCN-01 (100 nM) inhibited the phosphorylation of GSK-3 within 5–30 min (Fig. 6), similar to that caused by wortmannin, used as a control (albeit the response to wortmannin was faster). The mammalian target of rapamycin (mTOR, also known as FK506-binding protein 12-rapamycin associated protein [FRAP] or rapamycin and FKBP12 target-1 protein [RAFT]) is also known to play a critical role in the transduction of proliferative signals mediated through the PI3K/Akt signaling pathway, and thus represents a prime target for anti-cancer therapy development (28, 29). Indeed, treatment of HN6 cells with UCN-01 or wortmannin inhibited mTOR phosphorylation (Fig. 6). Both results support the conclusion that inhibition of the PI3K/Akt pathway by UCN-01 results in decreased phosphorylation of its downstream targets.

DISCUSSION

Current studies addressing the molecular mechanisms involved in HNSCC development and progression are focused on the interplay between the sequential inactivation of tumor suppressor proteins and the deregulation of signal transduction pathways involved in cell proliferation, survival, or death (3). These deregulated signaling routes in HNSCC include hyperactivity of EGF receptor (EGFR), mitogen-activated protein kinases, nuclear factor-κB, and signal transducers and activators of transcription 3 (11, 30–34). For example, Albanell *et al.* (30) showed that activated extracellular signal-regulated kinase 1/2 were detected in the majority of HNSCC, with the highest level of activation in advanced regional lymph node metastasis in correlation with EGFR/tumor growth factor α expression. The constitutive activation of signal transducers and activators of transcription 3 in HNSCC has also been extensively documented, either as a consequence of EGFR overactivation or because of a recently described autocrine/paracrine-activating loop mediated by interleukin 6 and other cytokines (32, 34). Recent IHC studies on SCC of the oral cavity showed that nuclear factor-κB and inhibitor of nuclear factor-κB kinase α were highly expressed in almost all SCC specimens but not in normal or dysplastic epithelium, suggesting that high expression levels of nuclear factor-κB and inhibitor of nuclear factor-κB kinase α may play a role in antiapoptotic signaling and thus contribute to the malignant behavior of HNSCC (35).

In this regard, during the course of mouse skin carcinogenesis studies, we have recently observed that the activation of Akt is a key step in the progressive alterations occurring in this experimental SCC model (9). The activity of Akt increased in parallel with the promotion stages of mouse skin carcinogenesis

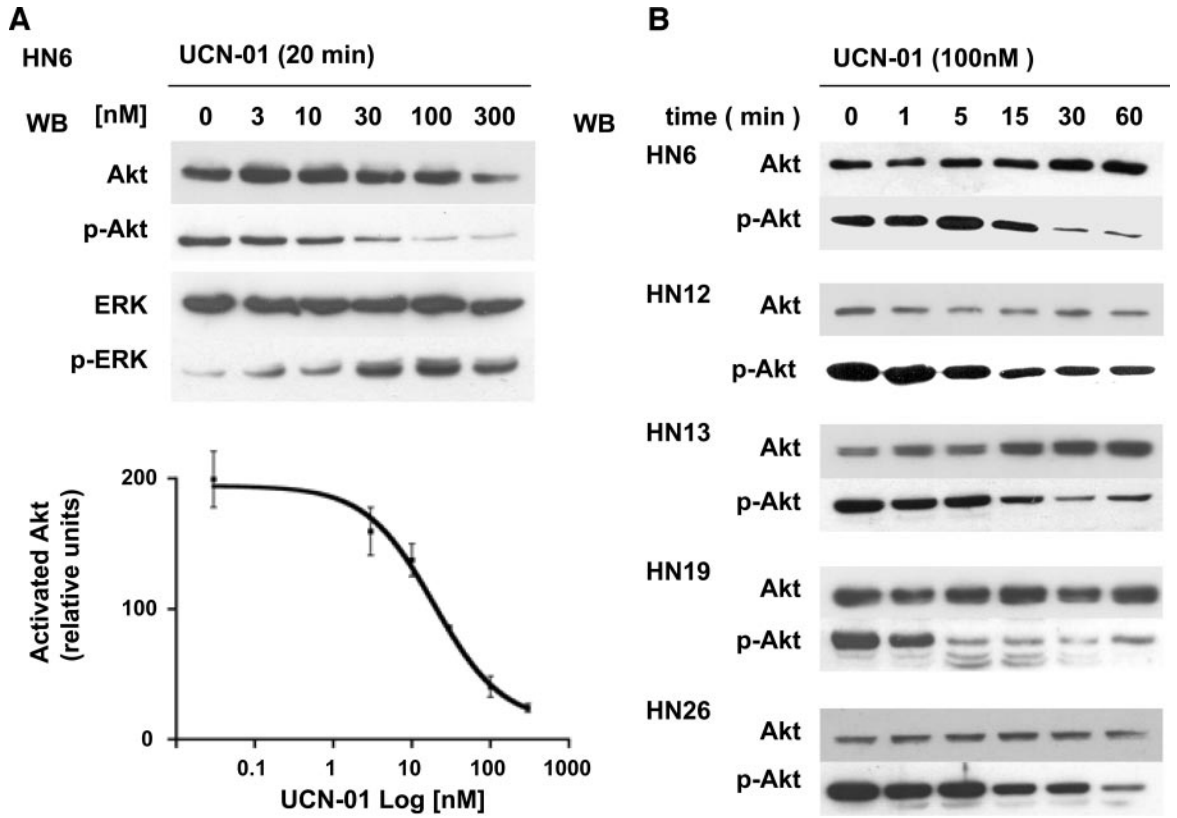

Fig. 5 Constitutively active Akt in squamous carcinoma of the head and neck (HNSCC) cells is inhibited by UCN-01. *A*, UCN-01 potently decreased the levels of activated phospho-Akt (*p*-Akt) in a dose-dependent manner in HNSCC cells. Lysates were prepared from serum-starved HNSCC cell lines treated with UCN-01 at the indicated concentration for 20 min. *p*-Akt levels in HN6 were assessed as indicated in "Materials and Methods" and plotted against UCN-01. Akt inhibition by UCN-01 (EC_{50} ~19 nM) correlated with the antiproliferative property of this antineoplastic agent in these cells when assessed by [^{3}H]thymidine incorporation (EC_{50} ~7 nM). In contrast, UCN-01 leads to activation of extracellular signal-regulated kinases (ERKs) as previously shown (26). *B*, inhibition of Akt activation by UCN-01 is an early event. HNSCC cells were treated with UCN-01 (100 nM) for the indicated time, and *p*-Akt and total Akt levels determined in cellular lysates by Western blotting (WB).

and remained high during the malignant conversion of papilloma to SCC. Furthermore, the expression of active Akt accelerates tumorigenesis and contributes to increased malignancy of SCC in mouse skin, as overexpression of Akt led to a more aggressive phenotype and showed increased proliferation with decreased apoptosis and differentiation (9). Although informative, these studies are limited by the use of *in vitro* kinase assays that determine Akt activity in lysates from whole tumors, thus restricting the analysis of the cell types contributing to Akt activity within the tumor mass. We now show that this enhanced Akt activity correlated well with the immune detection of active Akt in hyperplastic and malignant epithelial cells using phospho-specific antibodies that detect the activated state of Akt. Thus, this simple immunological approach reflected the increased activity of Akt during tumor progression. Active Akt localized mainly in the cytoplasm of the tumor cells, which also correlated with the increased Akt activity observed in cytoplasmic extracts when compared with nuclear extracts, although the ratio between nuclear and cytoplasmic activities increased during the process of tumor progression (9).

Although skin carcinogenesis models do not fully recapitulate the progression of human squamous carcinomas based on these observations, we investigated the status of Akt activity in human HNSCC. Our IHC results indicate that Akt activation is a frequent event that parallels the severity and progression stage of HNSCC. This status of Akt hyperactivity was also reflected in a large fraction (70%) of HNSCC-derived cell lines, irrespective of their status of activation of EGFR (34), mutational profile of *p53* (16), and level of expression of cell cycle inhibitors $p16^{INK4A}$, $p21^{WAF1}$, and $p27^{KIP1}$.

The signaling pathway leading to Akt activation begins with the activation of PI3Ks, either as a result of the stimulation of receptor tyrosine kinases such as EGFR, the stimulation of small GTPases related to Ras and Rac, the activation of cytokine receptors such as interleukins 2, 3, 4, 5, and 8, insulin, insulin-like growth factor, or the activation of receptors that signal through heterotrimeric G proteins (4). Once these multiple upstream pathways activate PI3Ks, these enzymes generate 3′-phosphoinositides such as PIP_3 in the membrane, which then recruit Akt and subsequently another PIP_3-sensitive kinase, PDK1. PDK1 phosphorylates Akt on Thr^{308} and Ser^{473}, thereby causing its activation (4, 5). In turn, PKB/Akt phosphorylates and regulates the function of multiple cellular proteins involved in processes that include proliferation and cell survival.

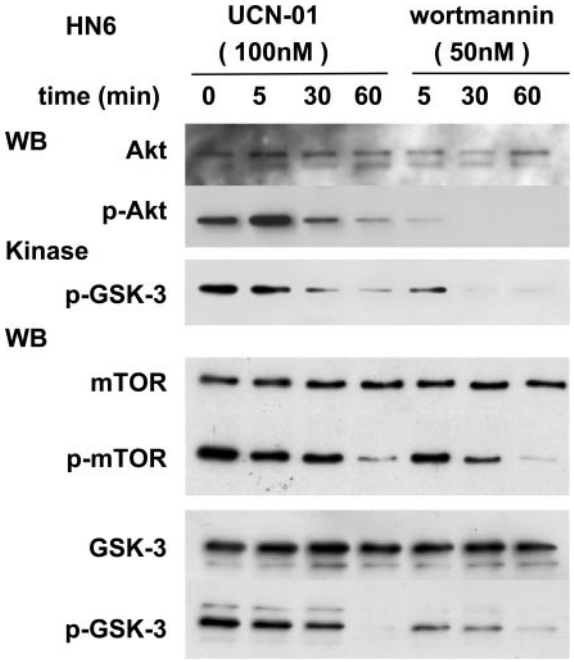

Fig. 6 Inhibition of downstream targets of Akt by UCN-01 in squamous carcinoma of the head and neck. HN6 cells were used as a representative squamous carcinoma of the head and neck cell line and treated with UCN-01 (100 nM) or wortmannin (50 nM) as a control for the indicated time. Levels of total and phosphorylated Akt (*p*-Akt) in cell lysates, as well as Akt *in vitro* kinase activity, were assessed as in Fig. 4. The phosphorylation status of endogenous glycogen synthase kinase-3 (p-GSK-3) and mTOR (*p*-mTOR) was determined by Western blotting (WB) using phospho-specific antibodies. Total levels of these proteins were also determined.

Whether the remarkable activation of Akt in HNSCC results from the dysregulation of a common, unique event or from multiple unrelated molecular mechanisms converging on PI3KPDK1 activation is at the present unknown. For example, overexpression of EGFR and its ligand, tumor growth factor α, is often observed in HNSCC (33), and thus, persistent activation of EGFR may lead to enhanced Akt activity. Interestingly, gene amplification of the PI3K-α locus, 3q26, and the consequent overexpression of the encoded PI3K catalytic subunit has been recently reported to represent a frequent event in HNSCC, which correlates with poor prognosis and patient survival (36). Thus, PI3K overexpression may contribute directly to the elevated Akt activity detected in HNSCC. Furthermore, based on the likely contribution of Akt to HNSCC progression, the PI3K-Akt signaling route may represent an attractive candidate as a target for therapeutic intervention in HNSCC. Of interest, although clinically useful Akt inhibitors are currently not available, recent biochemical reevaluation of the specificity and selectivity of commonly used protein kinase inhibitors led to the discovery that one derivative of staurosporine, UCN-01, can block PDK1 at low nM concentrations ($IC_{50} < 33$ nM), concentrations similar to or even lower than those required to block other kinases such as protein kinase Cs (4–30 nM) and Chk1 (IC_{50} ~600 nM). This compound is of particular interest because it inhibits cell growth in several *in vitro* and *in vivo* human tumor preclinical models. Furthermore, Phase I clinical trials of UCN-01 conducted in refractory neoplasms have shown that UCN-01 can be administrated safely (25). Although UCN-01 displays binding to human plasma proteins, free UCN-01 levels of ~110 nM, the level at which UCN-01 could potentially act on signaling molecules and DNA damage checkpoint proteins (37). Thus, based on this information, we can hypothesize that PDK1 may represent a biologically relevant target for UCN-01 *in vivo* and that part of its antitumor activities may be dependent on its ability to block the PDK1-Akt signaling pathway.

In particular for HNSCC, we recently have shown that UCN-01 displays potent antiproliferative properties in HNSCC cell lines, leading to cell apoptosis, and that in HNSCC tumor xenograft models, treatment with UCN-01 for 5 consecutive days leads to a sustained inhibition of tumor growth, even with only one cycle of UCN-01 treatment. These effects were associated with a high incidence of apoptosis in treated tissues, a decrease in cyclin D3, and an increase in $p27^{KIP1}$ levels. Our current studies indicate that UCN-01 administered at concentrations that cause cell cycle arrest (30–100 nM) can clearly inhibit the Akt pathway in HNSCC cell lines and that this is an early event because it occurs within the first 20–30 min of treatment. Thus, these observations, taken together with the frequent occurrence of Akt activation in HNSCCs and their derived cell lines, suggest that the Akt pathway may represent a key target for UCN-01 in this tumor type.

In summary, our findings suggest that Akt activation is a frequent event in HNSCC. Although increased levels of active Akt were associated with the malignant state, additional studies with large sample collections will be required to evaluate whether active Akt represents a marker of diagnostic or prognostic value in HNSCC patients. On the other hand, treatment with UCN-01 can inhibit growth in HNSCC cells and can down-regulate the *p*-Akt levels at very low concentrations that can be safely achieved in clinical settings. Taken together, these findings provide a rationale for the early clinical evaluation of novel Akt and PDK1 inhibitors in HNSCC patients, as well as the potential use of active, phosphorylated Akt, GSK-3, and mTOR levels as a surrogate biomarker to evaluate the activity of UCN-01 in tumor tissues in future trials.

REFERENCES

1. Landis SH, Murray T, Bolden S, Wingo PA. Cancer statistics, 1999. CA - Cancer J Clin 1999;49:8–31, 1.

2. Parkin DM, Pisani P, Ferlay J. Global cancer statistics. CA - Cancer J Clin 1999;49:33–64, 1.

3. Forastiere A, Koch W, Trotti A, Sidransky D. Head and neck cancer. N Engl J Med 2001;345:1890–1900.

4. Meier R, Hemmings BA. Regulation of protein kinase B. J Recept Signal Transduct Res 1999;19:121–8.

5. Vivanco I, Sawyers CL. The phosphatidylinositol 3-kinase AKT pathway in human cancer. Nat Rev Cancer 2002;2:489–501.

6. Stal O, Perez-Tenorio G, Akerberg L, et al. Akt kinases in breast cancer and the results of adjuvant therapy. Breast Cancer Res 2003;5: R37–44.

7. Itoh N, Semba S, Ito M, Takeda H, Kawata S, Yamakawa M. Phosphorylation of Akt/PKB is required for suppression of cancer cell apoptosis and tumor progression in human colorectal carcinoma. Cancer (Phila.) 2002;94:3127–34.

8. Arboleda MJ, Lyons JF, Kabbinavar FF, et al. Overexpression of AKT2/protein kinase Bbeta leads to up-regulation of beta1 integrins, increased invasion, and metastasis of human breast and ovarian cancer cells. Cancer Res 2003;63:196–206.

9. Segrelles C, Ruiz S, Perez P, et al. Functional roles of Akt signaling in mouse skin tumorigenesis. Oncogene 2002;21:53–64.

10. Coghlan LG, Gimenez-Conti I, Kleiner HE, et al. Development and initial characterization of several new inbred strains of SENCAR mice for studies of multistage skin carcinogenesis. Carcinogenesis (Lond.) 2000;21:641–6.

11. Cardinali M, Pietraszkiewicz H, Ensley JF, Robbins KC. Tyrosine phosphorylation as a marker for aberrantly regulated growth-promoting pathways in cell lines derived from head and neck malignancies. Int J Cancer 1995;61:98–103.

12. Patel V, Lahusen T, Leethanakul C, et al. Antitumor activity of UCN-01 in carcinomas of the head and neck is associated with altered expression of cyclin D3 and p27(KIP1). Clin Cancer Res 2002;8: 3549–60.

13. Lawlor MA, Alessi DR. PKB/Akt: a key mediator of cell proliferation, survival and insulin responses? J Cell Sci 2001;114:2903–10.

14. Powis G, Bonjouklian R, Berggren MM, et al. Wortmannin, a potent and selective inhibitor of phosphatidylinositol-3-kinase. Cancer Res 1994;54:2419–23.

15. Yeudall WA, Crawford RY, Ensley JF, Robbins KC. MTS1/CDK4I is altered in cell lines derived from primary and metastatic oral squamous cell carcinoma. Carcinogenesis (Lond.) 1994;15:2683–6.

16. Cardinali M, Kratochvil FJ, Ensley JF, Robbins KC, Yeudall WA. Functional characterization *in vivo* of mutant p53 molecules derived from squamous cell carcinomas of the head and neck. Mol Carcinog 1997;18:78–88.

17. Takahashi I, Asano K, Kawamoto I, Tamaoki T, Nakano H. UCN-01 and UCN-02, new selective inhibitors of protein kinase C. I. Screening, producing organism and fermentation J Antibiot (Tokyo) 1989;42:564–70.

18. Akinaga S, Gomi K, Morimoto M, Tamaoki T, Okabe M. Antitumor activity of UCN-01, a selective inhibitor of protein kinase C, in murine and human tumor models. Cancer Res 1991;51:4888–92.

19. Koh J, Kubota T, Migita T, et al. UCN-01 (7-hydroxystaurosporine) inhibits the growth of human breast cancer xenografts through disruption of signal transduction. Breast Cancer 2002;9:50–4.

20. Usuda J, Saijo N, Fukuoka K, et al. Molecular determinants of UCN-01-induced growth inhibition in human lung cancer cells. Int J Cancer 2000;85:275–80.

21. Shao RG, Shimizu T, Pommier Y. 7-Hydroxystaurosporine (UCN-01) induces apoptosis in human colon carcinoma and leukemia cells independently of p53. Exp Cell Res 1997;234:388–97.

22. Jai W, Yu C, Rahmani M, et al. Synergistic antileukemic interactions between 17-AAG and UCN-01 involve interruption of Raf/MEK- and Akt-related pathways. Blood 2003;102:1824–32.

23. Owa T, Yoshino H, Yoshimatsu K, Nagasu T. Cell cycle regulation in the G_1 phase: a promising target for the development of new chemotherapeutic anticancer agents. Curr Med Chem 2001;8:1487–503.

24. Sato S, Fujita N, Tsuruo T. Interference with PDK1-Akt survival signaling pathway by UCN-01 (7-hydroxystaurosporine). Oncogene 2002;21:1727–38.

25. Sausville EA, Arbuck SG, Messmann R, et al. Phase I trial of 72-hour continuous infusion UCN-01 in patients with refractory neoplasms. J Clin Oncol 2001;19:2319–33.

26. Yu C, Dai Y, Dent P, Grant S. Coadministration of UCN-01 with MEK1/2 inhibitors potently induces apoptosis in BCR/ABL+ leukemia cells sensitive and resistant to ST1571. Cancer Biol Ther 2002;1: 674–82.

27. Bakin AV, Tomlinson AK, Bhowmick NA, Moses HL, Arteaga CL. Phosphatidylinositol 3-kinase function is required for transforming growth factor beta-mediated epithelial to mesenchymal transition and cell migration. J Biol Chem 2000;275:36803–10.

28. Sekulic A, Hudson CC, Homme JL, et al. A direct linkage between the phosphoinositide 3-kinase-AKT signaling pathway and the mammalian target of rapamycin in mitogen-stimulated and transformed cells. Cancer Res 2000;60:3504–13.

29. Podsypanina K, Lee RT, Politis C, et al. An inhibitor of mTOR reduces neoplasia and normalizes p70/S6 kinase activity in Pten+/− mice. Proc Natl Acad Sci USA 2001;98:10320–5.

30. Albanell J, Codony-Servat J, Rojo F, et al. Activated extracellular signal-regulated kinases: association with epidermal growth factor receptor/transforming growth factor alpha expression in head and neck squamous carcinoma and inhibition by anti-epidermal growth factor receptor treatments. Cancer Res 2001;61:6500–10.

31. Ondrey FG, Dong G, Sunwoo J, et al. Constitutive activation of transcription factors NF-(kappa)B, AP-1, and NF-IL6 in human head and neck squamous cell carcinoma cell lines that express pro-inflammatory and pro-angiogenic cytokines. Mol Carcinog 1999;26:119–29.

32. Song JI, Grandis JR. STAT signaling in head and neck cancer. Oncogene 2000;19:2489–95.

33. Grandis JR, Melhem MF, Gooding WE, et al. Levels of TGF-alpha and EGFR protein in head and neck squamous cell carcinoma and patient survival. J Natl Cancer Inst (Bethesda) 1998;90:824–32.

34. Sriuranpong V, Park JI, Amornphimoltham P, Patel V, Nelkin BD, Gutkind JS. Epidermal growth factor receptor-independent constitutive activation of STAT3 in head and neck squamous cell carcinoma is mediated by the autocrine/paracrine stimulation of the interleukin 6/gp130 cytokine system. Cancer Res 2003;63:2948–56.

35. Nakayama H, Ikebe T, Beppu M, Shirasuna K. High expression levels of nuclear factor kappaB, IkappaB kinase alpha and Akt kinase in squamous cell carcinoma of the oral cavity. Cancer (Phila.) 2001;92: 3037–44.

36. Singh B, Stoffel A, Gogineni S, et al. Amplification of the 3q26.3 locus is associated with progression to invasive cancer and is a negative prognostic factor in head and neck squamous cell carcinomas. Am J Pathol 2002;161:365–71.

37. Sausville EA, Elsayed Y, Monga M, Kim G. Signal transduction-directed cancer treatments. Annu Rev Pharmacol Toxicol 2003;43:199–231.

Clinical Cancer Research

Persistent Activation of the Akt Pathway in Head and Neck Squamous Cell Carcinoma: A Potential Target for UCN-01

Panomwat Amornphimoltham, Virote Sriuranpong, Vyomesh Patel, et al.

Clin Cancer Res 2004;10:4029-4037.